International Journal of Minerals, Metallurgy and Materials
Volume 26, Number 4, April 2019, Page 467
https://doi.org/10.1007/s12613-019-1754-4

Biogenic amino acid methionine-based corrosion inhibitors of mild steel in acidic media

L.K.M.O. Goni, M.A. Jafar Mazumder, S.A. Ali, M.K. Nazal, and H.A. Al-Muallem

Chemistry Department, King Fahd University of Petroleum and Minerals, Dhahran 31261, Saudi Arabia
(Received: 29 June 2018; revised: 24 October 2018; accepted: 30 October 2018)

Abstract: *N*,*N*-Diallyl methionine ethyl ester hydrochloride **5** underwent alternating copolymerization with SO_2 via the Butler cyclopolymerization protocol in dimethyl sulfoxide (DMSO) to give water-soluble cycloterpolymer **6** with a ~1:1 molar ratio of sulfide and sulfoxide groups as a result of oxygen transfer from DMSO. Half of the sulfide groups in **6**, upon oxidation with H_2O_2, afforded polymer sulfoxide **7** and polymer sulfone **8.** The solution properties of these polymers were determined via a viscometric technique. The thermal stability of these polymers was determined by thermogravimetric analysis. The inhibition efficiency obtained from gravimetric mass loss, potentiodynamic polarization, and electrochemical impedance spectroscopy techniques agreed well with each other. The corrosion efficiencies increase with increasing concentration of the polymers. At a polymer concentration of 175 μM, the maximum inhibition efficiency of copolymer compounds **6**–**8** was determined to be 92%, 97%, and 95%, respectively. The synthesized polymer compounds acted as mixed-type inhibitors. Polymer compound **7** adsorbed onto the metal surface via chemisorption and physisorption and obeyed Langmuir, Temkin, and Freundlich adsorption isotherms. Analyses by X-ray photoelectron spectroscopy and scanning electron microscopy–energy-dispersive X-ray spectroscopy indicated that the adsorbed polymers formed a thin film on the metal surface and prevented further corrosive attack.

Keywords: cyclopolymerization; methionine; methionine sulfoxide; methionine sulfone; diallylamine salt; corrosion inhibition

1. Introduction

Organic inhibitor molecules owe their ability to inhibit the corrosion of mild steel to the presence of heteroatoms, whose effectiveness is known to increase in the order O < N < S < P [1]. Our objective was to exploit the presence of S, N, and O in the amino acid methionine (**1**) (Fig. 1) to mitigate mild steel corrosion in hostile environments. Third-period elements such as S and P, being more polarizable than first- and second-period elements, can utilize their electron lone pairs to form coordinate-type bonds with the vacant *d*-orbitals of Fe or Fe^{2+} on the surface of steel [2], thereby interfering with anodic or cathodic reactions responsible for corrosion [3–4]. For mild-steel corrosion, methionine **(1)** (Fig. 1), having three different heteroatoms, at concentrations of 25, 149, and 746 ppm, has been reported to impart inhibition efficiency (IE) of 47% in 0.1 M HCl [5] at 25°C, 89% in 1 M HCl [6] at 30°C, and 54.8% in 0.5 M H_2SO_4 [7] at 30°C, respectively. Methionine methyl ester hydrochloride at a concentration of 923 ppm has been shown to achieve an IE of 81.2% in 1 M HCl [8] at 30°C. The IEs of methionine (**1**), methionine sulfoxide (**2**), and methionine sulfone (**3**) at respective concentrations of 149, 165, and 181 ppm have been determined to be 79%, 85%, and 88%, respectively, against copper corrosion in 1 M HNO_3 at 30°C [9].

The previous discussion evinced that the use of low-cost, nontoxic methionine as an attractive green corrosion inhibitor has, at best, achieved modest success. However, we anticipate that the inclusion of methionine residues in a polymeric backbone might lead to its ability to better cover the surface and protect against attack by corrosive media. In fact, the literature includes reports demonstrating that polymers with multiple adsorption sites provide better IE than their monomeric analogs [10–12]. In this context, we explored the possible utilization of Butler's cyclopolymerization protocol [13–15] in the synthesis of polymers containing the residues of biogenic amino acid methionine (Fig. 1). The protocol involving diallylammonium salts has etched an impor-

Corresponding authors: M.A. Jafar Mazumder E-mail: jafar@kfupm.edu.sa; S.A. Ali E-mail: shaikh@kfupm.edu.sa
© University of Science and Technology Beijing and Springer-Verlag GmbH Germany, part of Springer Nature 2019

tant place in the synthesis of numerous industrially significant ionic polymers [13–15]. Poly(diallyldimethylammonium chloride), the simplest cyclopolymer synthesized using this protocol, has been the subject of more than 1000 publications and patents, and more than 1.6×10^4 t of this product are sold per year for water purification and personal care formulations [13]. The macromolecule having a five-membered-ring skeleton of pyrrolidine motifs embedded in the backbone is considered the eighth major polymer architecture of synthetic high polymers [16–17]. Diallylammonium salts have also been reported to undergo copolymerization with sulfur dioxide to form a wide variety of alternating copolymers [18–20]. In one such copolymerization, methionine (a biogenic amino acid)-derived diallylamine salt **5**/SO_2 copolymerization in dimethyl sulfoxide (DMSO) as a solvent afforded alternate copolymer **6**, in which almost half of the sulfide groups had been oxidized to sulfoxide groups via O exchange with DMSO. Copolymer **6** was then transformed into polymer sulfoxide **7** and polymer sulfone **8** by treatment with H_2O_2 at 20 and 35°C, respectively (Fig. 1) [21]. Notably, polymers **6**–**8** contain residues of methionine, methionine sulfoxide, and methionine sulfone while keeping intact the original motifs of nitrogen with unquenched valency.

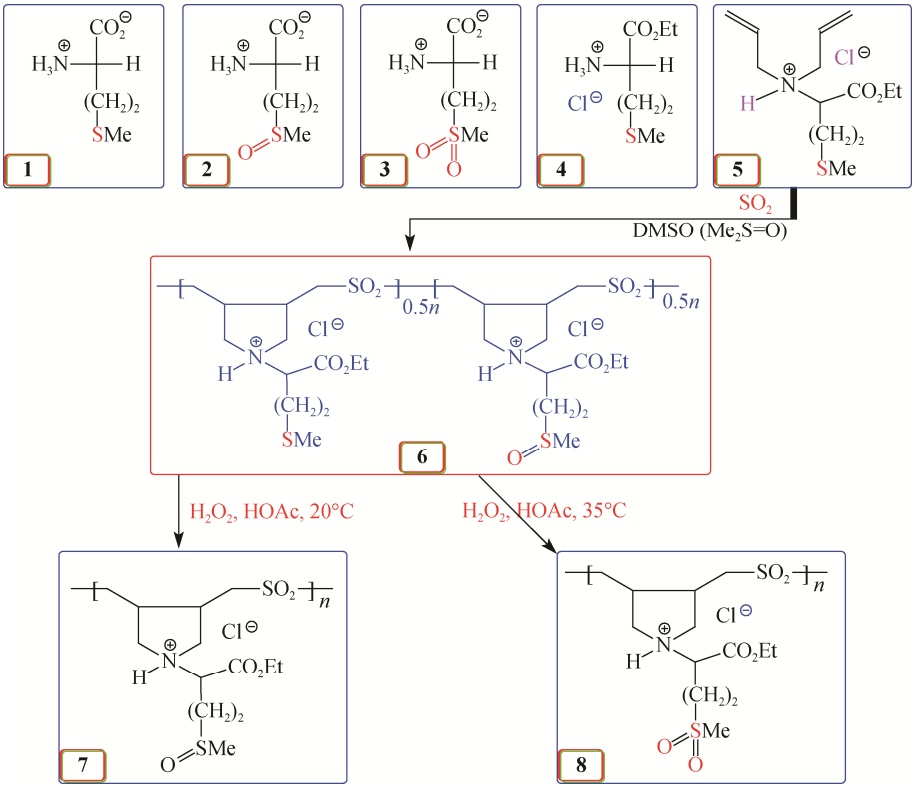

Fig. 1. Amino acid methionine-based cyclopolymer corrosion inhibitors containing sulfide, sulfoxide, and sulfone motifs.

The cost, safety, health, and environmental aspects associated with corrosion are of great concern to both industry and society. A recent study by National Association of Corrosion Engineers (NACE) International titled "International Measures of Prevention, Application and Economics of Corrosion Technology (IMPACT)" estimates the global cost of corrosion at US$2.5 trillion in 2016 [22]. Therefore, even a meager improvement of 1% IE amounts to enormous savings. Herein, we report the inhibition of corrosion of mild steel in 1 M HCl by polymers **6**–**8** with methionine residues in each repeating unit. In addition to demonstrating their efficacy as inhibitors, our study reveals the comparative efficacies of the sulfide, sulfoxide, and sulfone motifs.

2. Experimental

2.1. Materials

Ethyl ester hydrochloride of L-methionine (**4**), allyl bromide, and azoisobutyronitrile (AIBN) were purchased from Fluka Chemie AG, Switzerland. AIBN was recrystallized from $CHCl_3$–EtOH. Hydrogen peroxide (35wt% in water), hydrochloric acid (37wt% solution in water), acetic acid, and potassium carbonate (K_2CO_3) were purchased from BDH Chemical Ltd. (Poole, England) and used as received. DMSO, dried over CaH_2 overnight, was distilled at 0.4 mm Hg pressure and 64–65°C. All of these chemicals were used for the synthesis of the polymers.

2.2. Physical methods

The structural composition was determined by Fourier transform infrared (FT-IR) spectroscopy (Perkin Elmer 16F PC FTIR), and nuclear magnetic resonance (NMR) spectroscopy (JEOL LA 500 MHz). The elemental composition was determined with an elemental analyzer (Perkin Elmer, model 2400). The viscosity values of synthesized compounds were determined with a Ubbelohde viscometer (viscometer constant 0.005317 $mm^2 \cdot s^{-2}$). Thermogravimetric analysis (TGA) was performed using Pt/Pt–Rh (type R) thermocouples under N_2 (flow rate 50 $mL \cdot min^{-1}$) in an SDT thermogravimetric analyzer (TA Instruments Q600, New Castle, DE, USA); the temperature was increased at 10°C·min^{-1}) from 20 to 800°C. The electrochemical measurements were performed on a computer-controlled potentiostat–galvanostat (Auto Lab, Booster 10A-BST707A).

2.3. Synthesis

L-Methionine **1**-derived monomer of hydrochloride salts **5** and its SO_2-copolymer [poly(*N*,*N*-diallylmethionine ethyl ester hydrochloride-sulfur dioxide)-*ran*-(*N*,*N*-diallylmethionine sulfoxide ethyl ester hydrochloride-sulfur dioxide)] **6** were synthesized as described in our previous report [21]. The SO_2-sulfide/sulfoxide copolymers **6** were converted to their sulfoxide [poly(*N,N*-diallylmethionine sulfoxide ethyl ester hydrochloride-*alt*-sulfur dioxide)] **7** and sulfone [poly(*N,N*-diallylmethionine sulfone ethyl ester hydrochloride-*alt*-sulfur dioxide)] **8** analogs according to the procedure described in the litertaure [23].

2.4. Specimens

Corrosion inhibition tests by gravimetric and electrochemical measurements in 1 M HCl solution were performed using coupons prepared from mild steel with the following composition (wt%): C (0.089), Mn (0.34), Cr (0.037), Ni (0.022), Mo (0.007), Cu (0.005), V (0.005), P (0.010), and Fe (99.47). The flag-shaped mild-steel coupons (thickness: 1 mm) were used in electrochemical measurements. The stem of the flag (approximately 3 cm) was insulated with Araldite paint (RS, Saudi Arabia). The remaining area was approximately 1 cm^2 and provided an exposed area of 2 cm^2. The mild steel specimens were abraded with emery papers (100–1500 grit) and then degassed with acetone, washed with deionized water, dried in hot air at room temperature, and stored in a desiccator before use.

2.5. Solutions

A solution of 1 M HCl was prepared from concentrated HCl (37wt%) using double-distilled de-ionized water. The corrosion inhibition tests were performed in 1 M HCl solution in the presence of polymer compounds at the required concentrations. Inhibition tests carried out in the absence of a polymer compound were considered blanks.

2.6. Gravimetric measurements

The mild-steel coupons with almost equal sizes and masses were used to determine the inhibition efficiency via gravimetric mass-loss measurements. Mild steel coupons (2.5 cm × 2.0 cm × 0.1 cm) were immersed in 250 mL of 1 M HCl for 6 h in the absence or presence of polymer compounds **6–8** at 60°C. After the time elapsed, the steel coupons were cleaned by wiping with tissue paper, washed with distilled deionized water, and dried in a vacuum oven to a constant mass.

The inhibition efficiency (η_1) was calculated by the follow equation:

$$\eta_1 = \frac{W_b - W_i}{W_b} \times 100\% \quad (1)$$

where W_b and W_i represent mass loss in the absence or presence of polymer molecule, respectively.

The average relative mass loss of the mild-steel coupons was determined from three individual measurements. The average mass losses in percentage deviated within the range 0.5%–2.0%.

2.7. Electrochemical measurements

2.7.1. Open-circuit potential (OCP) versus time

The steady OCP was defined to be the value of the OCP when it does not change with time. Therefore, to determine the steady OCP, the effect of immersion time (0–60 min) of mild-steel coupons on their OCP was studied. A 1 M HCl solution was used as the blank, and two different concentrations (1.00 and 175 μM) of polymer compounds **6–8** prepared in 1 M HCl solution were investigated. The measurement results at various immersion times (Fig. 2) show that the OCP values became stable with negligible change at approximately 30 min.

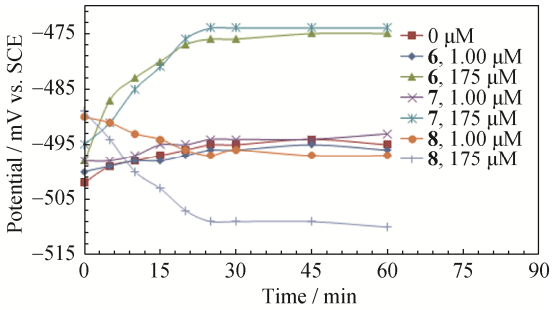

Fig. 2. Variation of the OCP of mild steel as a function of its immersion time in 1 M HCl solutions containing different concentrations (1.00 and 175 μM) of inhibitors 6–8 at 60°C.

2.7.2. Tafel extrapolations

The Tafel experiments were performed in a three-electrode electrochemical cell system. A mild-steel coupon was used as the working electrode, a 5-mm diameter graphite rod was used as the auxiliary electrode, and a saturated calomel electrode (SCE) was used as the reference electrode. The stable OCP of the working electrode was obtained after the mild steel coupon had been immersed for 30 min. All three electrodes were immersed in the absence or presence of polymer compounds **6–8** in 1 M HCl (250 mL) solution at 60°C, which was considered as a test solution. A potentiostat–galvanostat (Auto Lab, Booster 10A-BST707A, Eco Chemie, Netherlands) coupled with computer-controlled NOVA (version 1.8) software was used to record the polarization curves with a current off 1 A. The scan was performed in a potential window of ±250 mV around the corresponding OCP at a scan rate of 0.5 $mV \cdot s^{-1}$. Eq. (2) was used to calculate the inhibition efficiencies (η_2) based on the corrosion current density:

$$\eta_2 = \frac{I_{\text{CorrBlank}} - I_{\text{CorrInhibitor}}}{I_{\text{CorrBlank}}} \times 100\% \quad (2)$$

where $I_{\text{CorrBlank}}$ is the corrosion current in the absence of a polymer inhibitor and $I_{\text{CorrInhibitor}}$ is the corrosion current in the presence of one of the polymer inhibitors.

2.7.3. Linear polarization resistance (LPR) method

By recording the current versus potential in a range of ±10 mV around the E_{corr} under the same conditions described in section 2.7.2 (Tafel extrapolations), the LPR for polymer compounds **6–8** at different concentrations (0, 1.75, 4.85, 8.75, 17.5, 26.2, 35.2, and 175 μM) was measured. The surface coverage (θ) which correlated to the inhibition efficiencies (η_3) was calculated from the polarization resistance in the absence (R_p) and presence (R'_p) of polymer compounds using Eq. (3):

$$\eta_3 = \theta = \frac{R'_p - R_p}{R'_p} \times 100\% \quad (3)$$

2.7.4. Electrochemical impedance spectroscopy (EIS)

The same three-electrode system described in section 2.7.2 (Tafel extrapolations) was used to perform the electrochemical impedance experiments. A freshly prepared solution (250 mL) containing different concentrations of polymer compounds in 1 M HCl at 60°C was used. A frequency ranging from 100 kHz to 50 mHz and an amplitude of 10 mV were employed to record the Nyquist and Bode plots at the corresponding OCP. The resultant experimental data were subsequently fitted with the electrochemical equivalent circuit that provided the smallest deviation.

2.8. Surface characterization

2.8.1. X-ray photoelectron spectroscopy (XPS)

The XPS analysis was performed with an X-ray photoelectron spectrometer (Thermo Scientific, model Escalab 250 Xi). The Avantage software was used to process the data. The C 1s peak at 285.4 eV was used as a reference peak. The XPS spectra were deconvoluted using a nonlinear least-squares algorithm with a Shirley baseline and a combined Gaussian–Lorentzian peak shape.

2.8.2. Scanning electron microscopy (SEM) and energy-dispersive X-ray spectroscopy (EDX)

The surface morphology of the corroded (blank) and inhibited (presence of polymer) metal surface was observed by field-emission scanning electron microscopy (FESEM, Lyra 3, Tescan, Czech Republic) with accelerating voltages of 20–30 kV. In addition, an EDX spectrometer (Oxford Inc., UK) fitted with an X-Max detector was used to determine the chemical compositions and map the level of homogeneity of the metal surfaces. The SEM images were captured after the steel samples had been immersed at 60°C for 6 h in the absence (0 μM) or presence of a polymer inhibitor (175 μM).

3. Results and discussion

3.1. Polymer synthesis

The polymer SO_2-sulfide/sulfoxide (1:1) copolymer **6** [21] and its sulfoxide derivative **7** and sulfone derivative **8** were synthesized following the published literature procedure [23]. The intrinsic viscosity (η) values of cyclocopolymers **6**, **7**, and **8** were obtained from viscosity measurements of 1%–0.125% solutions in 0.1 M NaCl at 30°C using the Mark–Huggins viscosity relationship and were determined to be 0.137, 0.151, and 0.143 $dL \cdot g^{-1}$, respectively. These low viscosity values of η indicate that the polymers have low molar masses. The TGA curves of copolymers **6–8**, as shown in Fig. 3, indicate that these copolymers are stable to 200°C.

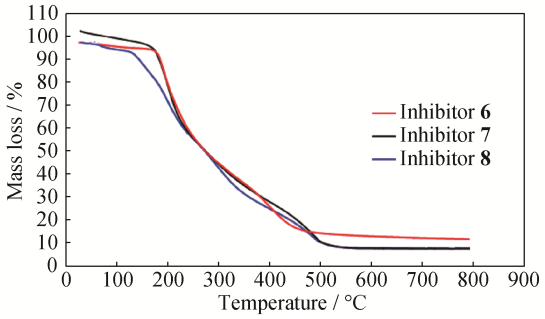

Fig. 3. TGA curves for corrosion inhibitors 6–8.

3.2. Corrosion gravimetric measurements

The results of the experiments obtained from gravimetric

mass-loss measurements after 6 h of immersion of the mild-steel coupons in the absence or presence of copolymers **6–8** in 1 M HCl (250 mL) at 60°C are presented in Table 1. Each set of experiments was carried out three times to obtain the average mass-loss results. The gravimetric mass-loss study indicated that the inhibition efficiency (η_1) values were 93.0%, 96.8%, and 95.7% at a concentration of 175 μM of ester-functionalized cyclocopolymers **6**, **7**, and **8**, respectively, whereas the η_1 values were 90.8%, 93.1%, and 85.0%, respectively, at a polymer concentration of ~13 ppm (35.1 μM). The experimental results obtained from gravimetric studies also show that the inhibition efficiency increases with increasing concentration of the cyclocopolymers, reaching maximum values attributable to the formation of a polymer layer onto the mild-steel surface. Within the range of concentrations studied for these cyclocopolymers, the ester-functionalized cyclocopolymer with sulfoxide motifs, **7**, exhibited slightly better corrosion inhibition of the mild steel. The better performance of cyclocopolymer **7** for inhibiting the corrosion of mild steel might be due to the presence of sulfoxide motifs in its polymer structure.

3.3. Polarization measurements

The stable OCP values were obtained from the experiments of OCP versus time. Fig. 2 shows that the OCP in the absence or presence of the polymer molecules **6** or **7** slightly moved in the positive direction and became stable within a short time, producing the free corrosion potential E_{corr} of the mild-steel coupon. In the presence of polymer molecule **8** (1.00 μM), the OCP values slowly changed toward more negative values; at high polymer concentration (175 μM), the rate of change was slower with higher magnitude and reached the steady state after ~30 min. The magnitude of the E_{corr} shift in the positive direction with increasing polymer concentration. The shifting of E_{corr} toward the positive direction is attributed to the preferential adsorption of inhibitors onto the anodic sites of the metal surface.

Fig. 4 shows the Tafel potentiodynamic polarization curves for the mild steel in absence and presence of different concentrations (1.00 to 175 μM) of cyclocopolymers **6–8** in

Table 1. η_1[a] **for inhibitors 6, 7, and 8 obtained by gravimetric mass loss method for the inhibition of corrosion of mild steel at 60°C in 1 M HCl solution for 6 h**

Sample	η_1 at different concentrations of inhibitors / %							
	1.75 μM	4.85 μM	8.75 μM	17.5 μM	26.2 μM	35.1 μM	70.2 μM	175 μM
6	50.6	57.7	74.3	82.1	90.5	90.8	92.4	93.0
7	53.4	66.9	77.0	83.2	90.7	93.1	94.6	96.8
8	42.9	54.3	64.8	75.6	82.7	85.0	94.3	95.7

Note: [a] IE (i.e., η_1) = surface coverage θ.

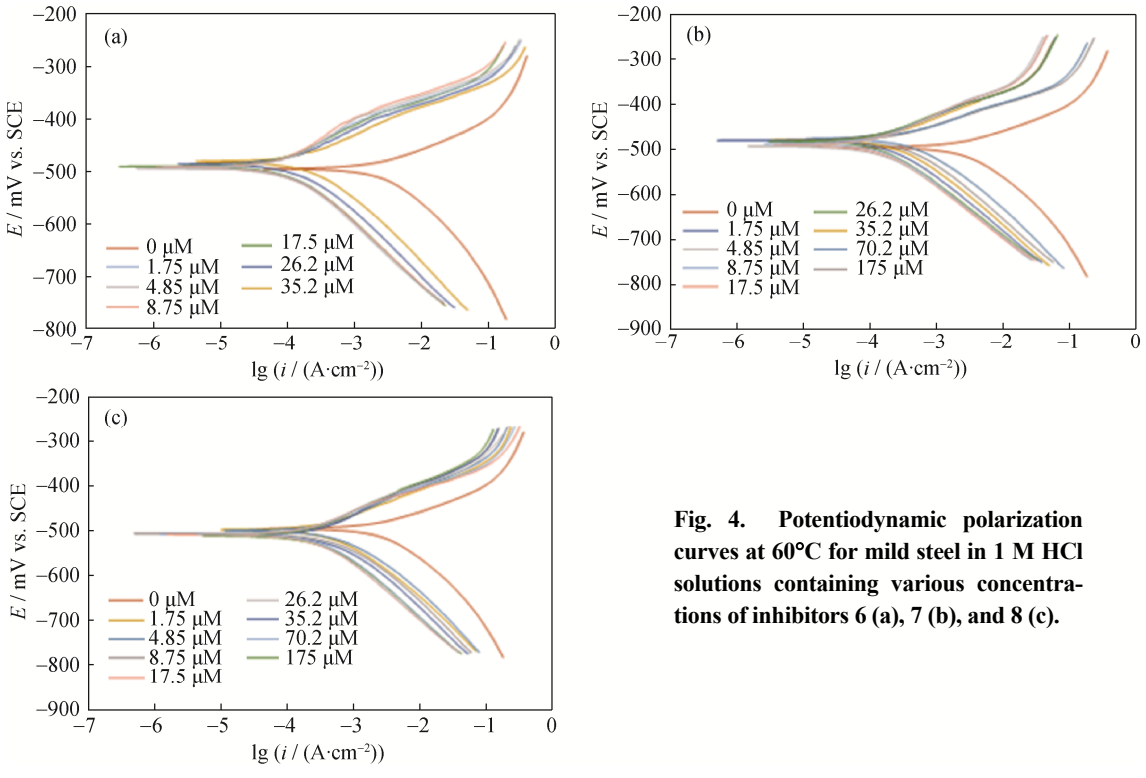

Fig. 4. Potentiodynamic polarization curves at 60°C for mild steel in 1 M HCl solutions containing various concentrations of inhibitors 6 (a), 7 (b), and 8 (c).

1 M HCl solution at 60°C. The extrapolation of linear segments of anodic and cathodic sides in the Tafel plots was used to obtain various electrochemical parameters such as the produced current density of corrosion (i_{corr}) and corrosion potential (E_{corr}) of mild-steel coupons; the results are summarized in Table 2. As shown in Table 2, the significant decrease in the i_{corr} is evidence of the inhibitive nature of the synthesized polymer compounds. The shifting of E_{corr} values in the positive or negative direction with a magnitude less than 85 mV suggests that they are mixed-type inhibitors, which mainly block the anodic and cathodic sites [24]. Thus, the inhibitors form a protective thin film on the metal surface instead of prompting the corrosion reactions. We also observed no substantial change or clear trend in the cathodic (β_c) and anodic (β_a) slopes, which suggests that the inhibition mechanism does not change with increasing the concentration of the inhibitors.

Table 2. Results of Tafel plots of a mild steel sample in 1 M HCl solutions containing inhibitors 6, 7, and 8 at different temperatures

Sample	Temperature / °C	Concentrations		Tafel					
		ppm	μM	E_{corr} / mV vs. SCE	β_a / (mV·dec^{-1})	β_c / (mV·dec^{-1})	i_{corr} / (μA·cm^{-2})	Corrosion rate / (mm·a^{-1})	η_2[a] / %
6	60	0	0	–495	73.8	–169	2465	28.6	—
		0.36	1.00	–494	64.4	–106	1506	17.5	38.9
		0.64	1.75	–494	58.8	–117	1395	16.2	43.4
		1.77	4.85	–492	70.8	–109	1038	12.0	57.9
		3.20	8.75	–491	79.9	–113	764	8.86	69.0
		6.40	17.5	–490	99.2	–127	486	5.64	80.3
		9.59	26.2	–486	89.1	–122	365	4.23	85.2
		12.9	35.2	–484	84.5	–110	335	3.89	86.4
		25.7	70.2	–481	92.3	–103	286	3.32	88.4
		64.0	175	–476	96.7	–106	177	2.05	92.8
7	50	0	0	–483	51.2	–117	505	5.85	—
		0.37	1.00	–478	59.8	–117	217	3.14	46.3
		0.65	1.75	–472	64.6	–119	245	2.84	51.5
		1.81	4.85	–467	82.1	–124	183	2.12	63.7
		3.27	8.75	–461	80.3	–108	126	1.46	75.0
		6.54	17.5	–455	71.4	–111	88.9	1.03	82.4
	60	0	0	–495	73.8	–169	2465	28.6	—
		0.37	1.00	–494	68.2	–112	1375	16.0	44.2
		0.65	1.75	–491	63.7	–104	1171	13.6	52.5
		1.81	4.85	–489	54.2	–112	858	9.95	65.2
		3.27	8.75	–486	75.7	–103	584	6.78	76.3
		6.54	17.5	–480	75.3	–118	431	5.01	82.5
		9.80	26.2	–480	94.1	–171	261	3.03	89.4
		13.2	35.2	–478	87.8	–111	187	2.17	92.4
		26.2	70.2	–478	85.0	–108	148	1.72	94.0
		65.4	175	–475	68.9	–101	76.4	0.89	96.9
	70	0	0	–498	60.9	–102	4508	52.3	—
		0.37	1.00	–493	65.2	–117	2466	28.6	45.3
		0.65	1.75	–486	67.4	–98.2	2200	25.5	51.2
		1.81	4.85	–485	84.3	–112	1650	19.1	63.4
		3.27	8.75	–477	92.1	–114	1253	14.5	72.2
		6.54	17.5	–472	85.5	–103	888	10.3	80.3
8	60	0	0	–495	73.8	–169	2465	28.6	—
		0.68	1.75	–497	75.2	–84.4	1496	17.4	39.3
		1.89	4.85	–499	75.3	–89.9	1156	13.4	53.1
		3.41	8.75	–506	85.4	–96.6	892	10.4	63.8
		6.82	17.5	–507	91.8	–99.7	636	7.38	74.2
		10.2	26.2	–507	96.5	–108	458	5.32	81.4
		13.7	35.2	–508	92.2	–112	397	4.60	83.9
		27.4	70.2	–510	89.1	–106	145	1.69	94.1
		68.2	175	–510	84.2	–105	126	1.46	94.9

Note: [a] Inhibition efficiency (IE), IE (i.e., η_2) = surface coverage θ.

The corrosion inhibition efficiencies of the synthesized polymer compounds for mild-steel coupons in 1 M HCl solution at 60°C, as obtained from Tafel and LPR experiments, are summarized in Tables 2 and 3, respectively. To our great satisfaction, cyclocopolymer **7**, which contains sulfoxide motifs, showed relatively better inhibition efficiency than cyclopolymers **6** and **8**. In addition, these results are in good agreement with the inhibition efficiencies calculated on the basis of mass-loss method (Table 1).

Table 3. Results of LPR method in 1 M HCl solutions containing inhibitors 6, 7, and 8 at different temperatures

Sample	Temperature / °C	Concentrations		LPR		
		ppm	μM	R'_p / (Ω·cm^2)	θ [a]	θ / %
6	60	0	0	2.38	—	—
		0.36	1.00	3.97	0.401	40.1
		0.64	1.75	4.34	0.452	45.2
		1.77	4.85	5.63	0.577	57.7
		3.20	8.75	7.63	0.688	68.8
		6.40	17.5	12.8	0.814	81.4
		9.59	26.2	17.0	0.860	86.0
		12.9	35.2	18.2	0.869	86.9
		25.7	70.2	20.0	0.881	88.1
		64.0	175	30.9	0.923	92.3
7	50	0	0	1.89	—	—
		0.37	1.00	3.57	0.471	47.1
		0.65	1.75	4.04	0.532	53.2
		1.81	4.85	5.49	0.656	65.6
		3.27	8.75	7.50	0.748	74.8
		6.54	17.5	11.4	0.835	83.5
	60	0	0	2.38	—	—
		0.37	1.00	4.50	0.471	47.1
		0.65	1.75	5.15	0.538	53.8
		1.81	4.85	7.23	0.671	67.1
		3.27	8.75	10.0	0.762	76.2
		6.54	17.5	14.6	0.837	83.7
		9.80	26.2	28.0	0.915	91.5
		13.2	35.2	32.2	0.926	92.6
		26.2	70.2	42.5	0.944	94.4
		65.4	175	70.0	0.966	96.6
	70	0	0	9.29	—	—
		0.37	1.00	16.8	0.446	44.6
		0.65	1.75	18.8	0.505	50.5
		1.81	4.85	25.9	0.641	64.1
		3.27	8.75	34.8	0.733	73.3
		6.54	17.5	49.4	0.812	81.2
8	60	0	0	2.38	—	—
		0.68	1.75	4.20	0.434	43.4
		1.89	4.85	5.28	0.549	54.9
		3.41	8.75	6.84	0.652	65.2
		6.82	17.5	9.64	0.753	75.3
		10.2	26.2	14.1	0.831	83.1
		13.7	35.2	15.8	0.849	84.9
		27.4	70.2	37.2	0.936	93.6
		68.2	175	50.6	0.953	95.3

Note: [a] IE (i.e., η_3) = surface coverage θ.

3.4. Impedance measurements

To better understand the corrosion inhibition performance, the EIS experiments were carried out after the coupons had been immersed in the test solution for 30 min. The recorded impedance data (Nyquist and Bode plots) of mild-steel coupon/solutions in the absence or presence of different concentrations (1.75 to 175 μM) of cyclocopolymers **6**–**8** were fitted using the Randles equivalent electrical/chemical circuit (the best-fit circuit) shown in Fig. 5. This simple circuit consists a solution resistance (R_s), a polarization resistance (R_p), and a constant phase element (CPE). The R_s value represents the potential drop between the mild-steel coupon as a working electrode and the reference electrode, and its value was calculated from the intersection of the fitted semicircle with the real (Z') axis at high frequency. The R_p values were obtained from the intersection of the semicircle with Z' axis at low frequency, to which other resistances such as the charge-transfer resistance and diffusion-layer resistance at the surface of the working electrode also contribute [25]. The net polarization resistance (R'_p) at the mild-steel coupon was calculated using Eq. (4), and its value was later used to calculate the inhibition efficiencies (η_4) based on the EIS using Eq. (3).

$$R'_p = R_p - R_s \quad (4)$$

The CPE expresses the nonideal capacitance and the nonideal frequency response. It is commonly used in the electrochemical circuit to attain a better fit. The double-layer capacitance (C_{dl}) is related to the CPE by Eq. (5):

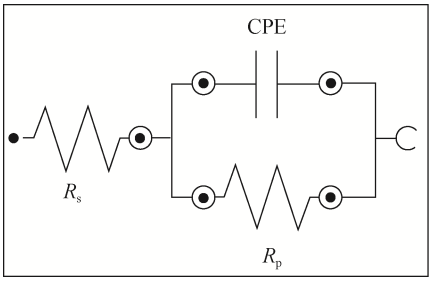

Fig. 5. Randles electrical/chemical equivalent circuit diagram used to model the metal/solution interface. R_s—Solution resistance; R_p—Polarization resistance; CPE—Constant phase element.

$$C_{dl} = \mathrm{CPE}(\omega)^{n-1} \quad (5)$$

where ω is the angular frequency (radians) at the maximum imaginary part of the impedance and n is the surface heterogeneity.

Table 4 summarizes the normalized EIS data for the corrosion of a mild-steel sample in 1 M HCl solutions containing

Table 4. Impedance parameters for the corrosion of a mild steel sample in 1 M HCl solutions containing inhibitors 6, 7, and 8 at 60°C

Sample	Concentrations		R_s / (Ω·cm^2)	R_p / (Ω·cm^2)	CPE[a] / (μF·cm^{-2})	n	R'_p / (Ω·cm^2)	η_4 / %
	ppm	μM						
	0	0	0.373	1.963	922	0.989	1.590	—
	0.64	1.75	0.479	3.537	566	0.905	3.058	48.0
	1.77	4.85	0.485	4.050	492	0.919	3.565	55.4
	3.20	8.75	0.447	5.837	348	0.846	5.390	70.5
6	6.40	17.5	0.436	9.077	335	0.827	8.641	81.6
	9.59	26.2	0.430	15.87	301	0.793	15.44	89.7
	12.9	35.2	0.128	16.52	262	0.722	16.39	90.3
	25.7	70.2	0.292	18.57	203	0.669	18.28	91.3
	64.0	175	0.334	19.96	197	0.554	19.63	91.9
	0	0	0.373	1.963	922	0.989	1.590	—
	0.65	1.75	0.433	3.759	465	0.941	3.326	52.2
	1.81	4.85	0.368	5.100	317	0.801	4.732	66.4
	3.27	8.75	0.362	7.157	325	0.716	6.795	76.6
7	6.54	17.5	0.126	8.910	311	0.658	8.784	81.9
	9.80	26.2	0.005	15.60	366	0.646	15.59	89.8
	13.2	35.2	0.419	20.05	247	0.780	19.63	91.9
	26.2	70.2	0.303	28.19	391	0.844	27.89	94.3
	65.4	175	0.330	44.10	207	0.835	44.17	96.4
	0	0	0.373	1.963	922	0.989	1.590	—
	0.68	1.75	0.510	3.256	546	0.896	2.746	42.1
	1.89	4.85	0.447	3.889	406	0.771	3.442	53.8
	3.41	8.75	0.474	4.878	343	0.758	4.404	63.9
8	6.82	17.5	0.521	6.805	309	0.840	6.284	74.7
	10.2	26.2	0.391	9.477	312	0.815	9.086	82.5
	13.7	35.2	0.532	10.54	305	0.847	10.01	84.1
	27.4	70.2	0.462	26.96	329	0.869	26.50	94.0
	68.2	175	0.557	30.55	252	0.875	29.99	94.7

Note: [a]Double layer capacitance (C_{id}) and coating capacitance (C_c) are usually modelled with a constant phase element (CPE) in modeling an electrochemical phenomenon.

different concentrations of inhibitors **6–8** at 60°C. The EIS fitting results show that the *n* values are less than 1, which is attributed to the poor homogeneity of the mild-steel surface. With increasing concentration of the polymer compounds, the R'_p values increased and the values of CPE decreased as a result of increasing thickness of the adsorbed polymer; this increasing polymer thickness eventually led to an increase of the inhibition efficiency, which reached 96.4% in the case of 175 μM polymer compound **7**. The lower *n* values at the higher concentrations of cyclocopolymers **6–8** are attributed to their increased adsorption onto the metal surface, which leads to an increase in the heterogeneity of the metal surface. The results obtained from the EIS study are consistent with the results of the gravimetric mass loss, LPR experiments, and Tafel plot.

The Nyquist and Bode plots are shown in Figs. 6–8 for different concentrations (1.75 to 175 μM) of polymers **6–8**. The inset in Fig. 6 shows the magnified Nyquist plots corresponding to the blank and to the experiments with low polymer concentrations. The Nyquist plots in Fig. 6 clearly demonstrate that the diameter of the semi-circle increases with increasing inhibitor concentration, which represents an increase in the thickness of the formed protective layer on the surface of the mild-steel electrode in response to the adsorption of the inhibitor compounds. The Bode magnitude plots (Fig. 7) for polymers **7** and **8** imply an increase in the R_p with increasing polymer concentration. The Bode phase angle plots (Fig. 8) for polymers **6–8** show an increase in the angle value at intermediate frequency with increasing inhibitor concentration, which demonstrates decreasing capacitance at the surface of the mild-steel electrode, resulting in a decrease of the local dielectric constant as well as an increase in the amount of inhibitors adsorbed onto the mild-steel coupon surface.

3.5. Adsorption isotherms

The inhibition effectiveness depends on the ability of inhibitor molecules to adsorb onto the mild-steel surface. To elucidate the adsorption mechanism of the synthesized polymer compounds, their adsorption thermodynamics were studied and the four most common adsorption isotherms

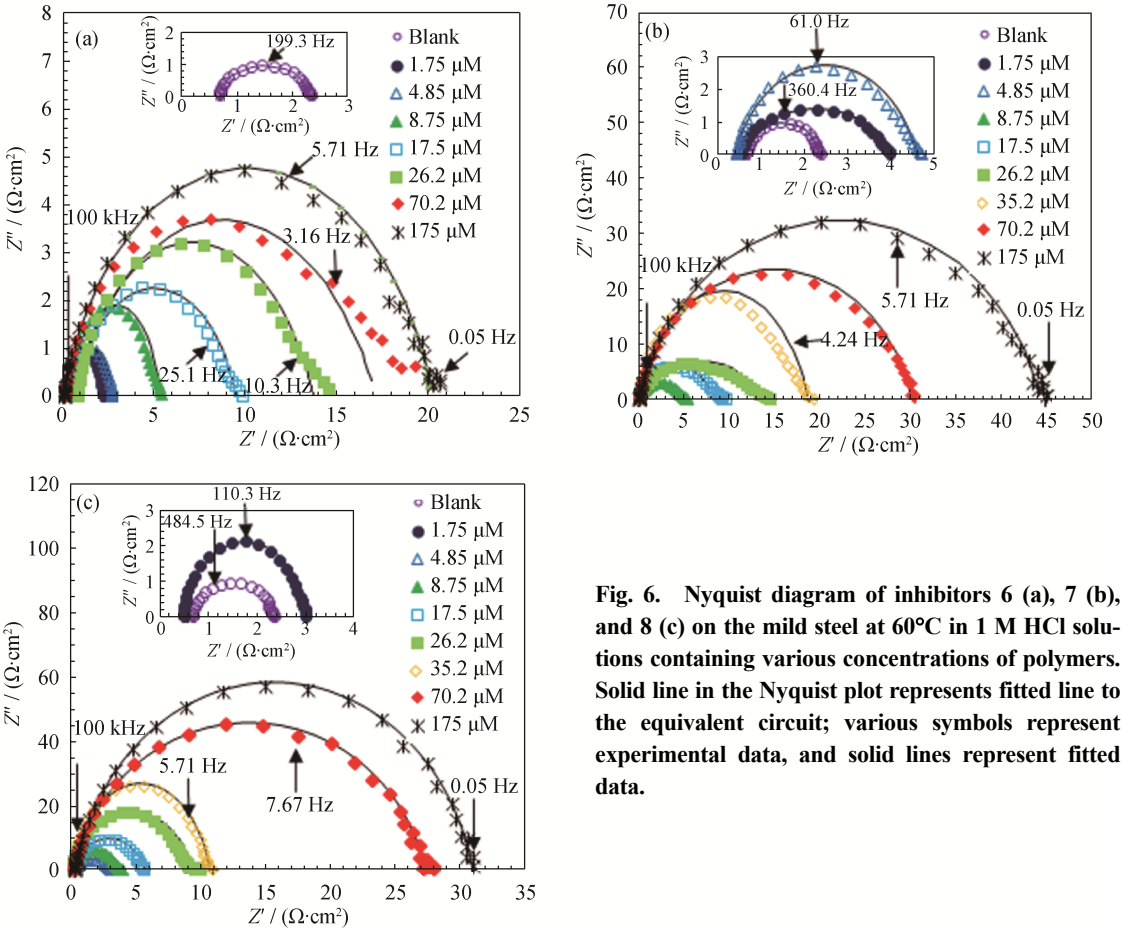

Fig. 6. Nyquist diagram of inhibitors 6 (a), 7 (b), and 8 (c) on the mild steel at 60°C in 1 M HCl solutions containing various concentrations of polymers. Solid line in the Nyquist plot represents fitted line to the equivalent circuit; various symbols represent experimental data, and solid lines represent fitted data.

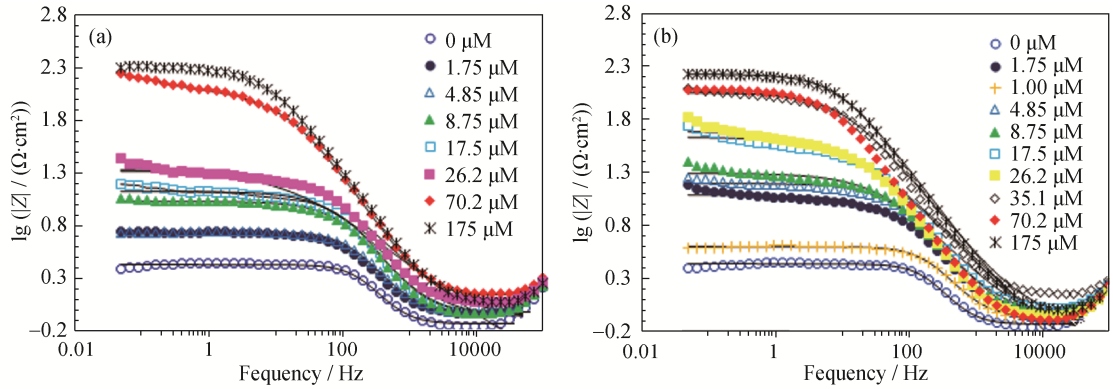

Fig. 7. Bode magnitude plots of inhibitors 6 (a), 7 (b), and 8 (c) on the mild steel at 60°C in 1 M HCl solutions containing various concentrations of polymers. Various symbols represent experimental data, and solid lines represent fitted data.

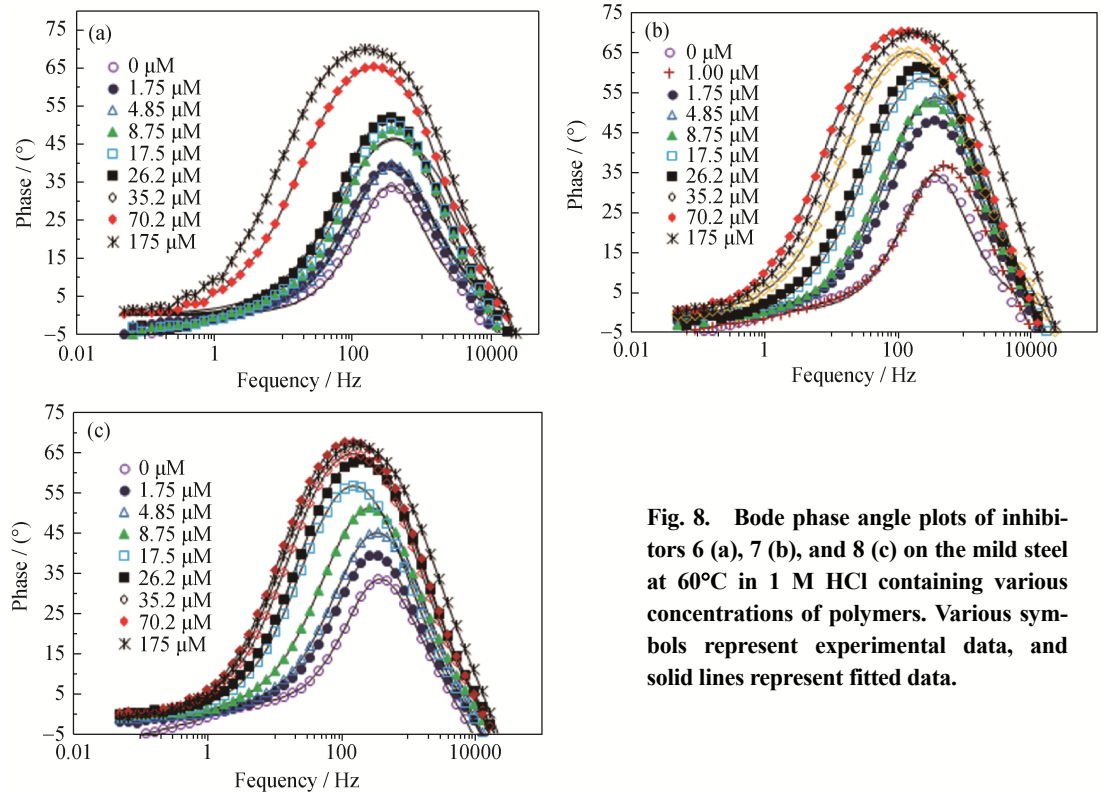

Fig. 8. Bode phase angle plots of inhibitors 6 (a), 7 (b), and 8 (c) on the mild steel at 60°C in 1 M HCl containing various concentrations of polymers. Various symbols represent experimental data, and solid lines represent fitted data.

(i.e., Freundlich, Langmuir, Frumkin, and Temkin's isotherms) describing the relationship between surface coverage (θ) and the bulk low concentration of inhibitor (C) (Eqs. (6)–(9)) [26] were tested using the linear least-squares method; the results are shown in Fig. 9.

Freundluich: $\theta = K_{ads}C^n$ (6)

Langmuir: $\theta/(1-\theta) = K_{ads}C$ (7)

Frumkin: $K_{ads}C = [\theta/(1-\theta)]\, e^{-2\alpha\theta}$ (8)

Temkin: $K_{ads}C = e^{f\theta}$ (9)

where K_{ads} and n are constants for a given adsorbate and adsorbent at a particular concentration; α and f are the interaction parameters.

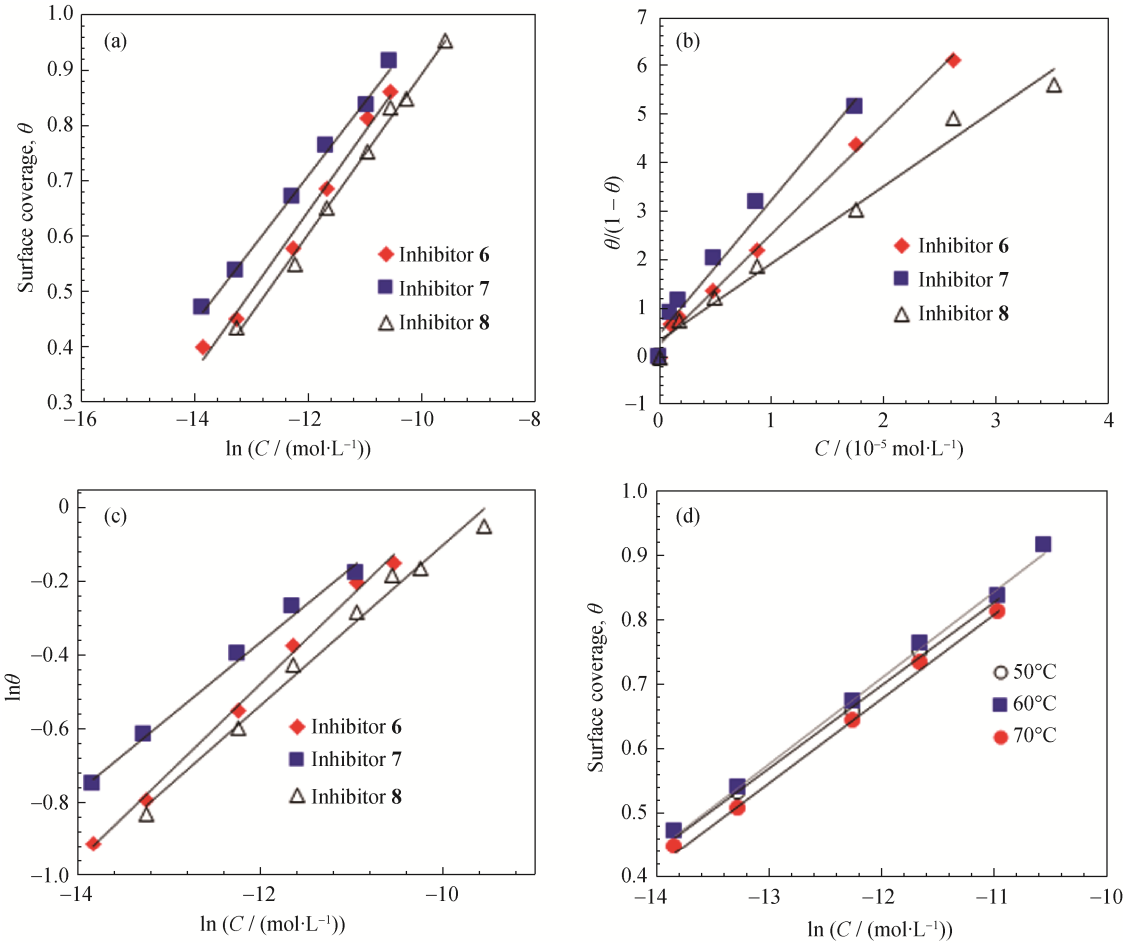

Fig. 9. (a) Temkin adsorption isotherm plots, (b) Langmuir adsorption isotherm, and (c) Freundlich adsorption isotherm for the adsorption of inhibitors 6–8 at 60°C; (d) Temkin adsorption isotherm for the adsorption of inhibitor 7 at various temperatures onto the surface of mild steel.

The square correlation coefficients (R^2) and the value of the constant in the tested isotherm models for polymers **6–8** at different temperatures are tabulated in Table 5. The higher correlation coefficient values obtained from Langmuir, Freundlich, and Temkin isotherm models (Table 5) suggest that the adsorption of inhibitors proceeds through a mixed chemisorption and physisorption mechanism, which means that both electrostatic and chemical interactions between the metal surface and the polymer compounds contribute to the adsorption process. To further explore the adsorption mechanism, the thermodynamic parameters (i.e., free energy ($\Delta G^{\ominus}_{ads}$) was calculated from Eq. (10), and enthalpy ($\Delta H^{\ominus}_{ads}$) and the entropy of adsorption ($\Delta S^{\ominus}_{ads}$)) were calculated using Eq. (11):

Table 5. Square of coefficient of correlation (R^2) and values of the constants in the adsorption isotherms of Temkin, Frumkin, Langmuir, and Freundlich in the presence of inhibitors 6, 7, and 8 in 1 M HCl solution (LPR data used for the isotherm)

Sample	Temperature / °C	Temkin (R^2, f)	Langmuir (R^2)	Frumkin (R^2, a)	Freundlich (R^2, n)
6	60	0.9883, 6.9	0.9981	0.8452, –0.2	0.9966, 0.2
7	50	0.9975, 7.8	0.9992	0.9522, –0.2	0.9977, 0.2
	60	0.9973, 7.5	0.9942	0.9796, –0.2	0.9930, 0.2
	70	0.9976, 7.7	0.9926	0.9764, –0.2	0.9946, 0.2
8	60	0.9952, 6.9	0.9873	0.8655, –0.2	0.9879, 0.2

$$K_{ads} = \frac{1}{55.5} \exp \frac{-\Delta G^{\ominus}_{ads}}{RT} \quad (10)$$

$$\Delta G^{\ominus}_{ads} = \Delta H^{\ominus}_{ads} - T\Delta S^{\ominus}_{ads} \quad (11)$$

The results are presented in Table 6.

The negative $\Delta G^{\ominus}_{ads}$ and $\Delta H^{\ominus}_{ads}$ values obtained from Figs. 10 and 11 indicate that the adsorption process is spontaneous and exothermic, respectively. Typically, the adsorption mechanism can be classified as physisorption, chemisorption, or mixed mechanism on the basis of the magnitude of $\Delta G^{\ominus}_{ads}$ and $\Delta H^{\ominus}_{ads}$. When the absolute value of $\Delta G^{\ominus}_{ads}$ is less than 20 kJ·mol^{-1} and the $\Delta H^{\ominus}_{ads}$ is less negative than −40 kJ·mol^{-1}, the adsorption process is described as physisorption. When the absolute value of $\Delta G^{\ominus}_{ads}$ is greater than 40 kJ·mol^{-1} and the $\Delta H^{\ominus}_{ads}$ is more negative than −100 kJ·mol^{-1}, the adsorption process can be classified as chemisorption; alternatively, a mixed mechanism would follow if the absolute value of $\Delta G^{\ominus}_{ads}$ is greater than 20 kJ·mol^{-1} but less than 40 kJ·mol^{-1} [27–30]. The calculated values of $\Delta G^{\ominus}_{ads}$ range from −43.5 and −46.8 kJ·mol^{-1}, and the $\Delta H^{\ominus}_{ads}$ for adsorption of synthesized polymer **7** was found to be −57.2 kJ·mol^{-1} (Table 6). These results suggest that adsorption is achieved through a mixed mechanism by the influence of the chemisorption mechanism. The π and non-bonded electrons induce the synthesized polymer molecules in different media to electrostatically and chemically interact with the anodic sites via overlapping the low-lying vacant *d*-orbitals of iron [31–32]. The positive value of $\Delta S^{\ominus}_{ads}$ (32 J·mol^{-1}·K^{-1}) for the adsorption of polymer compound **7** onto mild steel in 1 M HCl (Table 6, Fig. 10) is an indication that the randomness of the solid surface/inhibitor interface increases where the adsorbed inhibitor molecules displace the adsorbed water molecules on the surface of the mild steel.

Table 6. Values of the adsorption equilibrium constant from Langmuir adsorption isotherms and free energy, enthalpy, entropy changes of the mild steel dissolution in the presence of inhibitors 6, 7, and 8 in 1 M HCl solutions

Sample	Temperature / °C	K_{ads} [a] / (L·mol^{-1})	$\Delta G^{\ominus}_{ads}$ / (kJ·mol^{-1})	$\Delta H^{\ominus}_{ads}$ / (kJ·mol^{-1})	$\Delta S^{\ominus}_{ads}$ / (J·mol^{-1}·K^{-1})
6	60	13601929	–44.1	—	—
	50	37721678	–46.8		
7	60	32596030	–46.5	–57.2	32.0
	70	29435181	–46.2		
8	60	10665365	–43.5	—	—

Note: [a] K_{ads} obtained in L/mg was converted to L/mol.

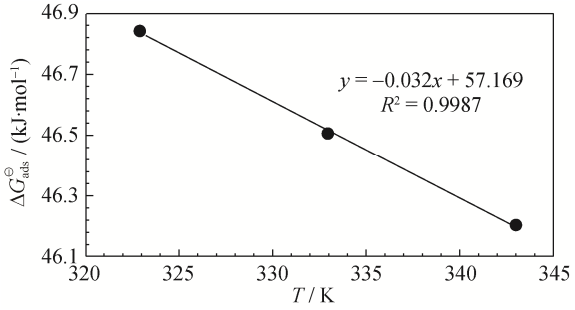

Fig. 10. Variation of $\Delta G^{\ominus}_{ads}$ versus *T* on mild steel in 1 M HCl solution containing inhibitor 7.

3.6. Surface analysis

XPS and SEM–EDX were used to further confirm the adsorption of polymer compounds onto the mild steel surface.

3.6.1. XPS analysis

The intensity versus binding energy plots recorded by XPS were used to analyze the elemental composition of the polymer compounds adsorbed onto the metal surface; the plots are presented in Figs. 11(a)–11(f). The XPS samples were prepared by immersing the mild-steel coupons for 6 h in a test solution containing 175 μM polymer at 60°C in 250 mL of 1 M HCl. The parameters obtained from the XPS analysis are depicted in Table 7. Figs. 11(a), 11(c), and 11(e) show the wide-scan XPS spectra of polymer compounds **6**–**8**. The signals of S 2p, N 1s, C 1s, and O 1s suggest that the polymer compounds, which contain N, C, O, and S, are present on the metal surface. The Fe 2p signal arises from the metal substrate and its corrosion product. The high-resolution XPS spectra of O 1s, C 1s, and Fe 2p are presented in Figs. 11(b), 11(d), and 11(f). The presence of O 1s peaks at 532.6, 532.0, and 530.2 eV in the spectrum in Fig. 11(b) is attributed to the fact that all of these studied polymers are of the type O=O, C–O, and O^{2-}, thereby implying an interaction between the polymer molecules and the oxide layer, which would promote the formation of a thin film on the metal surface [33–34]. The deconvoluted XPS profiles of the C 1s spectrum show a C–C aliphatic peak near 286.6 eV and C=O and C–N peaks near 285.4 eV (Fig. 11(d)). In the high-resolution XPS spectrum of Fe 2p, the intense peaks at approximately 716.2, 712.4, 709.8, and 707.3 eV are assigned to $Fe(OH)_x$, Fe^{3+} (2p), Fe^{2+}, and Fe^0 (2p), respectively (Fig. 11(f)).

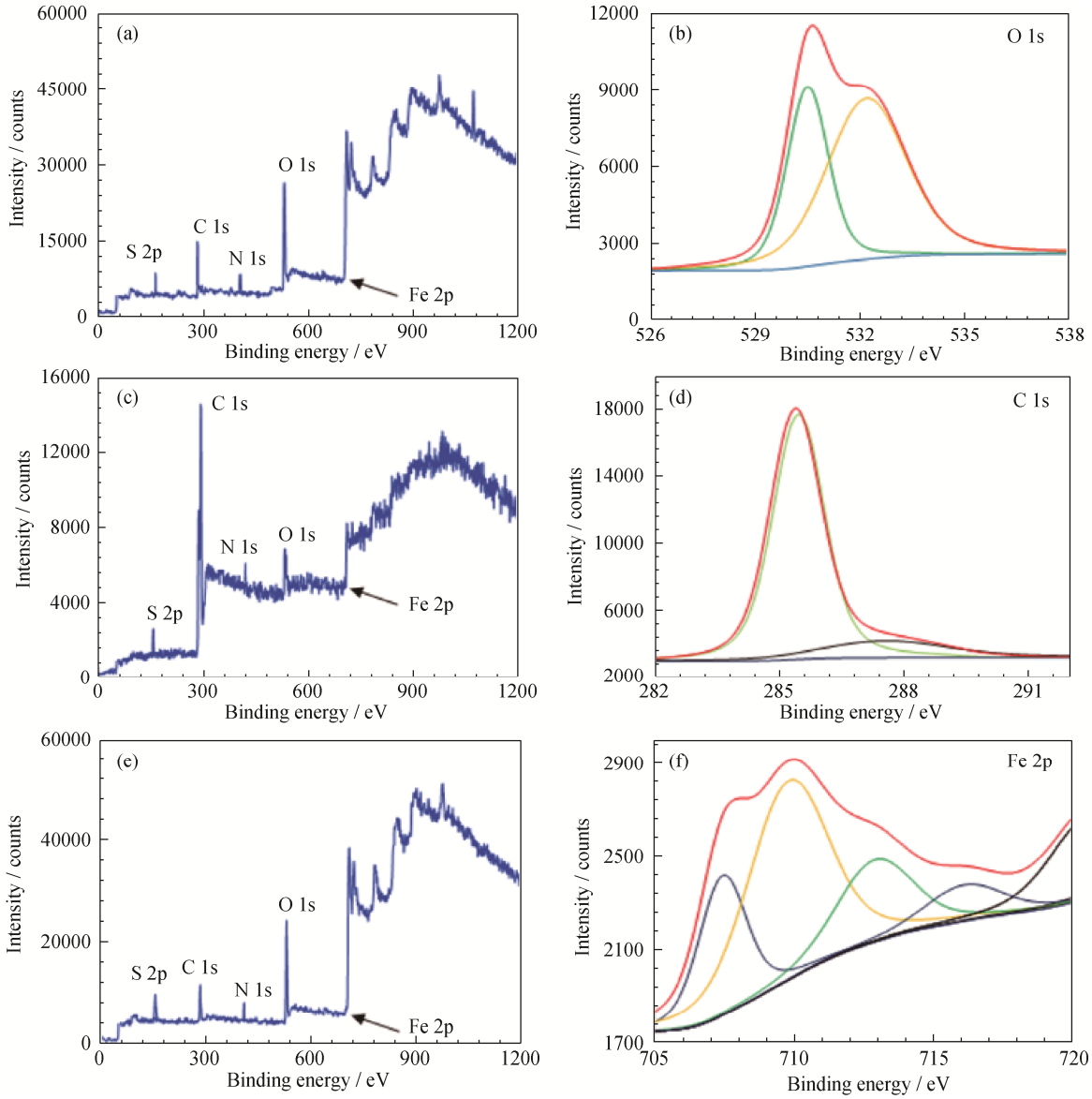

Fig. 11. XPS survey spectrum of inhibitors 6 (a), 7 (c), and 8 (e); XPS deconvoluted profiles of the O 1s of inhibitor 6 (b), the C 1s of inhibitor 7 (d), and the Fe 2p of inhibitor 8 (f) after the specimens were immersed in 1 M HCl at 60°C for 6 h (175 μM).

Table 7. XPS scan composition of mild steel coupon in 1 M HCl solutions containing inhibitors 6, 7, and 8 at 60°C

Peak	Approx. binding energy / eV	Composition / at%		
		6	**7**	**8**
C 1s	285.4	31.5	29.3	34.4
C 1s	286.6	19.4	18.7	13.2
O 1s	530.2	13.2	15.7	14.5
O 1s	532.0	—	—	30.6
O 1s	532.6	26.5	28.2	—
N 1s	400.2	3.98	1.86	3.09
Fe 2p	707.3	1.61	2.52	1.39
Fe 2p	709.8	2.98	1.99	0.97
Fe 2p	712.4	—	1.30	1.27
Fe 2p	716.2	—	—	0.43
Cl 2p	199.2	0.84	—	—

3.6.2. SEM–EDX analysis

The surface morphology of the mild steel in the absence and presence of polymer **7** after the specimens were immersed for 6 h in 1 M HCl were studied by SEM–EDX. The polished mild-steel surface without exposure to 1 M HCl (Fig. 12(a)) was used as reference. In the absence of polymer **7**, as shown in Fig. 12(b), the metal surface was severely damaged, the surface roughness and porosity were very high, and the surface was intensely corroded by the aggressive acid medium (1 M HCl). In presence of polymer **7** (175 μM), the effects of corrosion were suppressed; a smoother surface was detected (Fig. 12(c)) compared with the untreated surface (Fig. 12(b)). The mild-steel surface was relatively intact and smooth, suggesting that inhibitor

compound **7** protects the metal surface against aggressive corrosive media by forming a thin layer on the mild-steel surface. EDX analysis was carried out to further confirm the adsorption of polymer **7** onto the metal surface. A strong iron signal was detected for the reference (polished) sample (Fig. 12(d)); the iron and oxygen signals that appeared in the spectrum of the uninhibited sample could be due to the slow atmospheric oxidation and formation of Fe_2O_3 oxide films (Fig. 12(e)). As shown in Fig. 12(f), the spectrum of the inhibited surface showed a signal of iron with additional signals of carbon, nitrogen, and oxygen, implying the presence of adsorbed polymer that forms a protective layer on the metal surface to protect it from corrosive attack.

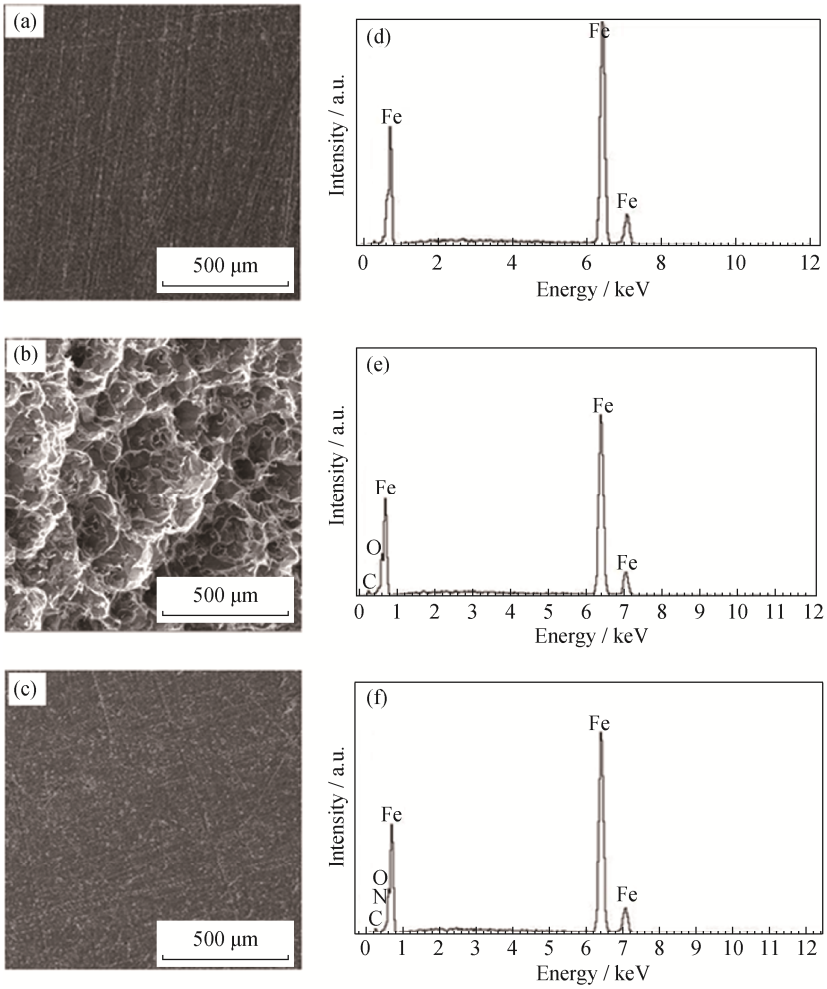

Fig. 12. SEM micrographs on the surface of the mild steel: (a) polished mild steel surface without exposure to 1 M HCl solution; (b) untreated mild steel after immersion for 6 h in 1 M HCl; (c) 175 μM of inhibitor 7 treated mild steel after immersion for 6 h in 1 M HCl . The corresponding EDX spectra are shown in (d), (e), and (f).

4. Conclusions

The inhibition effects of cyclocopolymers of sulfur dioxide and the biogenic amino acid methionine residue containing an ester functionality and sulfide, sulfoxide, or sulfone motifs in each alternating repeat unit were investigated for their feasibility as a corrosion inhibitor in acid media using gravimetric mass loss and electrochemical methods. From the present study, the following conclusions can be drawn.

(1) The synthesized cyclocopolymers showed excellent inhibition efficiency, inhibiting mild steel corrosion in 1 M HCl. In the presence of 175 μM cyclocopolymers **6**–**8**, the maximum corrosion efficiencies were determined to be 92%, 97%, and 95%, respectively.

(2) The inhibition efficiencies obtained from gravimetric mass loss, potentiodynamic polarization, and electrochemical impedance spectroscopy techniques are consistent with each other.

(3) The polymer compounds used in the present study act

as a mixed-type inhibitor; they adsorbed onto the metal surface via chemisorption and physisorption processes.

(4) The XPS and SEM–EDX analyses indicated that the adsorbed polymers formed a thin film on the metal surface and protected the surface from corrosive attack.

Acknowledgements

The authors gratefully acknowledge the research facilities provided by King Fahd University of Petroleum and Minerals (KFUPM) and the financial assistance of the Deanship of Scientific Research, KFUPM, Saudi Arabia through Internal project # IN131047.

References

[1] M.A. Kiani, M.F. Mousavi, S. Ghasemi, M. Shamsipur, and S.H. Kazemi, Inhibitory effect of some amino acids on corrosion of Pb–Ca–Sn alloy in sulfuric acid solution, *Corros. Sci.*, 50(2008), No. 4, p. 1035.

[2] V.S. Sastri, *Corrosion Inhibitors: Principles and Applications*, Wiley, New York, 1998.

[3] R.W. Revie and H.H. Uhlig, *Corrosion and Corrosion Control: An Introduction to Corrosion Science and Engineering*, 4th Ed., Wiley-Interscience, New York, 2008.

[4] B.D.B. Tiu and R.C. Advincula, Polymeric corrosion inhibitors for the oil and gas industry: Design principles and mechanism, *React. Funct. Polym.*, 95(2015), p. 25.

[5] S. Zor, F. Kandemirli, and M. Bingul, Inhibition effects of methionine and tyrosine on corrosion of iron in HCl solution: Electrochemical, FTIR, and quantum-chemical study, *Prot. Met. Phys. Chem. Surf.*, 45(2009), No. 1, p. 46.

[6] P. Shanmugasundaram, T. Sumathi, G. Chandramohan, and G.N.K. Ramesh-Bapu, Corrosion inhibition study of is: 1062 grade A - low carbon steel in 1 M HCl by L-Methionine -weight loss, ICP-OES and SEM-EDX studies, *Int. J. Curr. Res.*, 5(2013), No. 8, p. 2183.

[7] E.E. Oguzie, Y. Li, and F.H. Wang, Corrosion inhibition and adsorption behavior of methionine on mild steel in sulfuric acid and synergistic effect of iodide ion, *J. Colloid Interface Sci.*, 310(2007), No. 1, p. 90.

[8] B. Hammouti, A. Aouniti, M. Taleb, M. Brighli, and S. Kertit, L-Methionine methyl ester hydrochloride as a corrosion inhibitor of iron in acid chloride solution, *Corrosion*, 51(1995), No. 6, p. 411.

[9] K.F. Khaled, Corrosion control of copper in nitric acid solutions using some amino acids–A combined experimental and theoretical study, *Corros. Sci.*, 52(2010), No. 10, p. 3225.

[10] M.A.J. Mazumder, H.A. Al-Muallem, S.A. Ali, and M.K. Estaitie, Cyclopolymer containing residues of methionine and synthesis and uses thereof, U.S. patent, No. US9556301B1, 2017.

[11] Y.N. Wang, C.F. Dong, D.W. Zhang, P.P. Ren, L. Li, and X.G. Li, Preparation and characterization of a chitosan-based low-pH-sensitive intelligent corrosion inhibitor, *Int. J. Miner. Metall. Mater.*, 22(2015), No. 9, p. 998.

[12] R. Bacskai, A.H. Schroeder, and D.C. Young, Hydrocarbon-soluble alkylaniline/formaldehyde oligomers as corrosion inhibitors, *J. Appl. Polym. Sci.*, 42(1991), p 2435.

[13] G.B. Butler, *Cyclopolymerization and Cyclocopolymerization*, CRC Press, Florida, 1992.

[14] P.K. Singh, V.K. Singh, and M. Singh, Zwitterionic polyelectrolytes: A review, *E-Polymers*, 2007, No. 030, p. 1.

[15] W. Jaeger, J. Bohrisch, and A. Laschewsky, Synthetic polymers with quaternary nitrogen atoms—Synthesis and structure of the most used type of cationic polyelectrolytes, *Prog. Polym. Sci.*, 35(2010), No. 5, p. 511.

[16] G.B. Butler, Cyclopolymerization, *J. Polym. Sci.*, *Part A*: *Polym. Chem.*, 38(2000), No. 8, p. 3451.

[17] V.S. Saji, A review on recent patents in corrosion inhibitors, *Recent Pat. Corros. Sci.*, 2(2010), p. 6.

[18] S.A. Ali and O.C.S. Al-Hamouz, Comparative solution properties of cyclocopolymers having cationic, anionic, zwitterionic and zwitterionic/anionic backbones of similar degree of polymerization, *Polymer*, 53(2012), No. 15, p. 3368.

[19] N.Y. Abu-Thabit, I.W. Kazi, H.A. Al-Muallem, and S.A. Ali, Phosphonobetaine/sulfur dioxide copolymer by Butler's cyclopolymerization process, *Eur. Polym. J.*, 47(2011), No. 5, p. 1113.

[20] S.A. Ali, Y. Umar, B.F. Abu-Sharkh, and H.A. Al-Muallem, Synthesis and comparative solution properties of single-, twin-, and triple-tailed associating ionic polymers based on diallylammonium salts, *J. Polym. Sci.*, *Part A*: *Polym. Chem.*, 44(2006), No. 19, p. 5480.

[21] H.A. Al-Muallem, M.A.J. Mazumder, M.K. Estaitie, and S.A. Ali, A novel cyclopolymer containing residues of essential amino acid methionine: Synthesis and application, *Iran. Polym. J.*, 24(2015), No. 7, p. 541.

[22] G. Koch, J. Varney, N. Thompson, O. Moghissi, M. Gould, J. Payer, *The NACE International Impact Study* [2018-04-20], http://impact.nace.org/.

[23] S.A. Ali, L.K.M.O. Goni, and M.A.J. Mazumder, Butler's cyclopolymerizaton protocol in the synthesis of diallylamine salts/sulfur dioxide alternate polymers containing amino acid residues, *J. Polym. Res.*, 24(2017), No. 11, p 184.

[24] S.Z. Duan and Y.L. Tao, *Interface Chemistry*, Higher Education Press, Beijing, 1990, p. 124.

[25] M. Erbil, The determination of corrosion rates by analysis of AC impedance diagrams, *Chim. Acta. Turc.*, 1(1988), No. 1, p. 59.

[26] P.C. Okafor, X. Liu, and Y.G. Zheng, Corrosion inhibition of mild steel by ethylamino imidazoline derivative in CO_2-saturated solution, *Corros. Sci.*, 51(2009), No. 4, p. 761.

[27] L. Larabi, Y. Harek, M. Traisnel, and A. Mansri, Synergistic influence of poly(4-vinylpyridine) and potassium iodide on inhibition of corrosion of mild steel in 1 M HCl, *J. Appl. Electrochem.*, 34(2014), No. 8, p. 833.

[28] T. Arsian, F. Kandemirli, E.E. Ebenso, I. Love, and H. Alemu, Quantum chemical studies on the corrosion inhibition of

some sulphonamides on mild steel in acidic medium, *Corros. Sci*., 51(2009), No. 1, p. 35.

[29] G.Y. Elewady, I.A. El-Said, and A.S. Fouda, Anion surfactants as corrosion inhibitors for aluminium dissolution in HCl solutions, *Int. J. Electrochem. Sci*., 3(2008), No. 2, p. 177.

[30] G.E. Badr, The role of some thiosemicarbozide derivatives as corrosion inhibitors for carbon steel in acidic media, *Corros. Sci*., 51(2009), No. 11, p. 2529.

[31] C.G. Dariva and A.F. Galio, *Corrosion Inhibitors – Principles, Mechanisms and Applications*, IntechOpen, UK, 2014.

[32] L. Afia, R. Salghi, L. Bammou, E. Bazzi, B. Hammouti, L. Bazzi, and A. Bouyanzer, Anti-corrosive properties of argan oil on C38 steel in molar HCl solution, *J. Saudi Chem. Soc*., 18(2014), No. 1, p. 19.

[33] O. Olivares-Xometl, N.V. Likhanova, M.A. Domínguez-Aguilar, J.M. Hallen, L.S. Zamudio, and E. Arce, Surface analysis of inhibitor films formed by imidazolines and amides on mild steel in an acidic environment, *Appl. Surf. Sci*., 252(2006), No. 6, p. 2139.

[34] M. Tourabi, K. Nohair, M. Traisnel, C. Jama, and F. Bentiss, Electrochemical and XPS studies of the corrosion inhibition of carbon steel in hydrochloric acid pickling solutions by 3,5-bis(2-thienylmethyl)-4-amino-1,2,4-triazole, *Corros. Sci*., 75(2013), p. 123.